Measurement report: Oxidation potential of water-soluble aerosol components in the southern and northern of Beijing

Wei Yuan[1], Ru-Jin Huang[1], Chao Luo[2], Lu Yang[1], Wenjuan Cao[1], Jie Guo[1], Huinan Yang[2]

[1]State Key Laboratory of Loess and Quaternary Geology, Center for Excellence in Quaternary Science and Global Change, Institute of Earth Environment, Chinese Academy of Sciences, Xi'an 710061, China.

[2]School of Energy and Power Engineering, University of Shanghai for Science and Technology, Shanghai 200093, China

Correspondence: Ru-Jin Huang (rujin.huang@ieecas.cn) and Huinan Yang (yanghuinan@usst.edu.cn)

Abstract

Water-soluble components have significant contribution to the oxidative potential (OP) of atmospheric fine particles ($PM_{2.5}$), while our understanding of water-soluble $PM_{2.5}$ OP and its sources, as well as its relationship with water-soluble components, is still limited. In this study, the water-soluble OP levels in wintertime $PM_{2.5}$ in the south and north of Beijing, representing the difference in sources, were measured with dithiothreitol (DTT) assay. The volume normalized DTT (DTT_v) in the north (3.5 ± 1.2 nmol min^{-1} m^{-3}) was comparable to that in the south (3.9 ± 0.9 nmol min^{-1} m^{-3}), while the mass normalized DTT (DTT_m) in the north (65 ± 28 pmol min^{-1} μg^{-3}) was almost twice that in the south (36 ± 14 pmol min^{-1} μg^{-3}). In both the south and north of Beijing, DTT_v was better correlated with soluble elements instead of total elements. In the north, soluble elements (mainly Mn, Co, Ni, Zn, As, Cd and Pb) and water-soluble organic compounds, especially light-absorbing compounds (also known as brown carbon), had positive correlations with DTT_v. However, in the south, the

29 DTT$_v$ was mainly related to soluble As, Fe and Pb. The sources of DTT$_v$ were further

30 resolved using the positive matrix factorization (PMF) model. Traffic-related

31 emissions (39%) and biomass burning (25%) were the main sources of DTT$_v$ in the

32 south, and traffic-related emissions (> 50%) contributed the most of DTT$_v$ in the north.

33 Our results indicate that vehicle emission was the important contributor to OP in

34 Beijing ambient PM$_{2.5}$ and suggest that more study is needed to understand the

35 intrinsic relationship between OP and light absorbing organic compounds.

36

37 **1 Introduction**

38   Atmospheric fine particulate matter (PM$_{2.5}$) pollution is one of the major global

39 environmental issues, affecting air quality, climate and human health (Huang et al.,

40 2014; Burnett et al., 2018; An et al., 2019; Zheng et al., 2020). The exposure to PM$_{2.5}$

41 was estimated to be responsible for 8.9 million deaths worldwide in 2015, of which

42 28% occurred in China (Burnett et al., 2018). Numerous studies have shown that

43 oxidative stress is one of the main mechanisms underlying the adverse effects of

44 PM$_{2.5}$ on human health (Chowdhury et al., 2019; Lelieveld et al., 2021; Yu et al.,

45 2022b). When entering the human body, PM$_{2.5}$ can induce the production of excessive

46 reactive oxygen species (ROS) (e.g., H$_2$O$_2$, $\cdot$OH and $\cdot$O$_2^-$), leading to cellular redox

47 imbalance and generating oxidative stress effects. The ability of PM$_{2.5}$ to cause

48 oxidative stress is defined as oxidative potential (OP).

49   The methods to determine the OP of PM$_{2.5}$ include cellular and acellular assays,

50 and acellular methods are more widely used than cellular methods (Charrier and

51 Anastasio, 2012; Xiong et al., 2017; Calas et al., 2018; Bates et al., 2019; Wang et al.,

52 2020b; Campbell et al., 2021; Oh et al., 2023). Among acellular methods, the

53 dithiothreitol (DTT) assay is extensively applied to determine the OP of ambient

54 particles (Charrier and Anastasio, 2012; Xiong et al., 2017; Liu et al., 2018; Wang et

55 al., 2020b; Puthussery et al., 2022; Wu et al., 2022a). DTT is a surrogate of cellular

56 reductants, and the consumption rate of DTT was used to assess the OP of PM$_{2.5}$.

57 Previous studies have shown that organic matters (e.g., water-soluble organic species

and PAHs) and some transition metals (e.g., Mn and Cu) are the important contributors to DTT consumption of $PM_{2.5}$ (Charrier and Anastasio, 2012; Verma et al., 2015; Bates et al., 2019; Wu et al., 2022a; Wu et al., 2022b). For example, Charrier and Anastasio (2012) measured the OP of $PM_{2.5}$ in San Joaquin Valley, California and reported that about 80% of DTT consumption was contributed by transition metals. Verma et al. (2015) measured the OP of water-soluble $PM_{2.5}$ in the southeastern United States and reported that about 60% of DTT activity was contributed by water-soluble organics. The mixtures of metals and organics may produce synergistic or antagonistic effects, such as $\cdot O_2^-$ produced from oxidation of DTT by quinones is more efficiently transformed to $\cdot OH$ in the presence of Fe, while the DTT consumption and $\cdot OH$ generation of quinones are reduced in the presence of Cu (Xiong et al., 2017; Yu et al., 2018; Bates et al., 2019).

A number of studies have investigated the OP of water-soluble components in $PM_{2.5}$, which show that the average water-soluble OP values in urban areas ranged from 0.1 to 10 nmol min^{-1} m^{-3} (Fang et al., 2016; Liu et al., 2018; Chen et al., 2019; Wu et al., 2022a; Yu et al., 2022a; Xing et al., 2023). Due to the complexity in chemical composition and sources of $PM_{2.5}$ that determine the OP levels, the sources of OP are also diverse (Verma et al., 2015; Bates et al., 2019; Tuet et al., 2019; Yu et al., 2019; Cao et al., 2021). Several studies have investigated the emission sources and ambient samples to identify the sources of OP (Tuet et al., 2019; Yu et al., 2019; Wang et al., 2020b; Cao et al., 2021), which include both primary and secondary sources. For example, Cao et al. (2021) measured the water-soluble OP of $PM_{2.5}$ samples from six biomass and five coal burning emissions in China, with average values of 4.5-7.4 and 0.5-2.1 pmol min^{-1} μg^{-1}, respectively. Tong et al. (2018) investigated the OP of secondary organic aerosols (SOA) from oxidation of naphthalene, isoprene and β-pinene with $\cdot OH$ or O_3, which were 104 ± 7.6, 48 ± 7.9 and 36 ± 3.1 pmol min^{-1} μg^{-1}, respectively. Verma et al. (2014) identified the sources of water-soluble OP of $PM_{2.5}$ in Atlanta, United States from June 2012 to September 2013 with positive matrix factorization (PMF) and chemical mass balance (CMB) methods, of which biomass

burning was the largest contributor. Wang et al. (2020b) quantified the sources of water-soluble OP of $PM_{2.5}$ in Xi'an, China in 2017 using PMF and multiple linear regression (MLR) methods, with significant contributions from secondary sulfates, vehicle emissions and coal combustion. Despite these efforts, comparative studies on the differences in pollution levels and sources of $PM_{2.5}$ OP in different districts are still limited.

In this study, the DTT activity of water-soluble matter in $PM_{2.5}$ samples collected simultaneously in the southern and northern of Beijing in January 2018 were measured. The concentration and light absorption of water-soluble organic carbon (WSOC), as well as the concentrations of 14 trace elements and 7 light-absorbing nitroaromatic compounds (NACs) were quantified. The sources of DTT activity were then identified with PMF model. The results acquired in this study provide a comparison of $PM_{2.5}$ OP in different districts of Beijing and its connection with organic compounds, trace elements and sources, which could be helpful for further study of the regional differences in the effects of $PM_{2.5}$ on human health.

2 Materials and methods

2.1 Sampling

Ambient 24 h integrated $PM_{2.5}$ filter samples were collected from January 1 to 31, 2018 simultaneously in the south (the Dingfuzhuang village (DFZ), Daxing district; 39.61°N, 116.28°E) and north (the National Center for Nanoscience and Technology (NCNT), Haidian district; 39.99°N, 116.32°E) of Beijing (Figure S1). The distance between the two sampling sites is about 42 km. The south site is surrounded by agricultural, industrial, and transportation areas, and the north site is surrounded by residential, transportation and commercial areas. $PM_{2.5}$ samples were collected on pre-baked (780 °C, 3 h) quartz-fiber filters (20.3 × 25.4 cm; Whatman, QM-A, Clifton, NJ, USA) using high-volume $PM_{2.5}$ samplers (1.13 m^{-3} min^{-1}; Tisch, Cleveland, OH, USA) which were placed on the roof of buildings at heights of about 5 m (south) and 20 m (north) above the ground. 31 samples were collected at each site. After collection, the

116 samples were wrapped in baked aluminum foils and stored in a freezer (−20 °C) until

117 further analysis.

2.2 Chemical analysis

119 The mass of $PM_{2.5}$ on the filter was measured by a digital microbalance with a

120 precision of 0.1 mg (LA130S-F, Sartorius, Germany) after 24-h equilibration at a

121 constant temperature (20-23 °C) and humidity (35-45%) chamber. Each filter was

122 weighted at least two times, and the deviations for blank and sampled filters among

123 the repetitions were less than 5 and 10 μg, respectively. The $PM_{2.5}$ mass concentration

124 was calculated by dividing the weight difference before and after sampling by the

125 volume of sampled air.

126 For WSOC analysis, one punch (1.5 cm^2 for concentration analysis and 0.526

127 cm^2 for light absorption measurement) of filter was taken from each sample and

128 extracted ultrasonically with ultrapure water (> 18.2 MΩ cm) for 30 min. After, the

129 extracts were filtered with a 0.45 μm PVDF pore syring filter to remove insoluble

130 substances. Finally, the concentration of WSOC was measured with a total organic

131 carbon-total nitrogen analyzer (TOC-L, Shimadzu, Japan; (Ho et al., 2015)) and the

132 light absorption of WSOC was measured by an UV-Vis spectrophotometer (300-700

133 nm; Ocean Optics, USA) equipped with a liquid waveguide capillary cell (LWCC-

134 3100, World Precision Instruments, Sarasota, FL, USA; (Yuan et al., 2020)). The

135 absorption coefficient (Abs) of WSOC was calculated according to formula S1 in the

136 Supporting Information (SI).

137 The total concentration and soluble fraction concentration of 14 trace elements

138 (i.e., Ti, V, Cr, Mn, Fe, Co, Ni, Cu, Zn, As, Sr, Cd, Ba, and Pb) were quantified by an

139 inductively coupled plasma mass spectrometer (ICP-MS, 7700x, Agilent Technologies,

140 USA), and the details are shown in the SI. For soluble fraction concentration analysis,

141 a punch of filter (47 mm diameter) was extracted with ultrapure water and then

142 centrifuged from residues. For total concentration analysis, another 47 mm diameter

143 filter of the same sample was used and digested with 10 mL HNO_3 and 1 mL HF at

144 180 °C for 12 h. The extracts were then heated and concentrated to ~ 0.1 mL, and

145 diluted to 5 mL with 2% HNO$_3$. Afterwards, the diluents were filtered with a 0.22 μm

146 PTFE pore syring filter and stored in a freezer (−4 °C) until further ICP-MS analysis.

147   The concentrations of organic markers (including levoglucosan, mannosan,

148 galactosan, hopanes (including 17α(H)-22,29,30-trisnorhopane, 17α(H),21β(H)-30-

149 norhopane, 17β(H),21α(H)-30-norhopane, 17β(H),21α(H)-hopane, 17β(H),21α(H)-

150 hopane and 17β(H),21α(H)-hopane), picene, phthalic acid, isophthalic acid and

151 terephthalic acid) and light-absorbing NACs (including 4-nitrophenol (4NP), 2-

152 methyl-4-nitrophenol (2M4NP), 3-methyl-4-nitrophenol (3M4NP), 4-nitrocatechol

153 (4NC), 3-methyl-5-nitrocatechol (3M5NC), 4-methyl-5-nitrocatechol (4M5NC) and

154 4-nitro-1-naphthol (4N1N)) were determined by a gas chromatograph–mass

155 spectrometer (GC-MS; Agilent Technologies, Santa Clara, CA, USA) following the

156 method described elsewhere (Wang et al., 2020a), and more details about the analysis

157 can be found in SI. All of the results reported in this study were corrected for blanks.

158 **2.3 Oxidative potential**

159   The DTT assay was applied to determine the oxidative potential of water-soluble

160 components in PM$_{2.5}$ according to the method by Gao et al. (2017). In brief, a quarter

161 of a 47 mm filter was ultrasonically extracted with 5 mL ultrapure water for 30 min

162 and then filtered with a 0.45 μm PVDF pore syring filter to remove insoluble

163 substances. Several studies have shown that ultrasonic treatment of samples can lead

164 to an increase in their OP values (Miljevic et al., 2014; Jiang et al., 2019), however,

165 there was also a study showed that the difference in OP values of water-soluble PM$_{2.5}$

166 measured by DTT assay was little for samples extracted by ultrasonic and shaking

167 (Gao et al., 2017). Consistent with the extraction methods for organic markers and

168 trace elements, ultrasonic method was used to extract samples for DTT analysis.

169 Afterwards, 0.5 mL of the extract was mixed with 1 mL of potassium phosphate

170 buffer (pH = 7.4) and 0.5 mL of 2 mM DTT in a brown vial, and then placed in a

171 water bath at 37 °C. Then, 20 μL of this mixture was taken at designated time

172 intervals (2, 7, 13, 20, and 28 min) and mixed with 1 mL trichloroacetic acid (TCA;

173 1% w/v) in another brown vial to terminate the reaction. Then, 0.5 mL of 5,5'-

174   dithiobis-(2-nitrobenzoic acid) (DTNB; 2.5 μM) and 2 mL of tris buffer (pH = 8.9)

175   were added to form 2-nitro-5-thiobenzonic acid (TNB) which has light absorption at

176   412 nm. Finally, the absorption of TNB was measured by a LWCC-UV-Vis. The DTT

177   consumption rate was quantified by the remaining DTT concentration at different

178   reaction times. Daily solution blanks and filter blanks were analyzed in parallel with

179   samples to evaluate the consistency of the system performance. Besides, for every 10

180   samples, one sample was chosen to be measured three times to check the

181   reproducibility, and the relative standard deviation was lower than 5%. Ambient

182   samples were corrected for filter blank. The DTT activities were normalized by the

183   volume of sampled air (DTT_v, nmol min^{-1} m^{-3}) and the mass concentration of $PM_{2.5}$

184   (DTT_m, pmol min^{-1} μg^{-1}).

185   Considering that for samples containing a significant amount of substances

186   whose DTT response is non-linear with $PM_{2.5}$ concentration (e.g., Cu, Mn), the DTT_m

187   value depends on the concentration of $PM_{2.5}$ added to the reaction solution (Charrier

188   et al., 2016). The response of DTT_m to $PM_{2.5}$ concentration added to the reaction

189   solution was analyzed using sample containing high concentrations of soluble Cu and

190   Mn (Figure S2). When the $PM_{2.5}$ concentration added to the reaction solution is less

191   than 150 μg mL^{-1}, the DTT_m response is greatly affected by the difference in added

192    $PM_{2.5}$ concentration; however, when the $PM_{2.5}$ concentration added to the reaction

193   solution is greater than 150 μg mL^{-1}, the DTT_m response is less affected by the

194   difference in $PM_{2.5}$ concentration (< 12%). In this study, the concentration of $PM_{2.5}$

195   added to the reaction solution of most samples from the two sites was greater than 150

196   μg mL^{-1} (ranged from 79 to 749 μg mL^{-1}, with an average of 409 ± 164 and 207 ± 95

197   μg mL^{-1} in the south and north, respectively), therefore, the difference in $PM_{2.5}$

198   concentration added to the reaction solution of different samples should had a

199   relatively small impact on the difference in DTT_m values of different samples. This

200   study did not consider the impact of metal precipitation in phosphate matrix on the

201   measured DTT values, as there is not a straightforward method to correct the artifact

202   caused by this phenomenon (Yalamanchili et al., 2023).

2.4 Source apportionment

The sources of DTT activities were identified and quantified using PMF model implemented by the multilinear engine (ME-2; (Paatero, 1997)) following the method described in our previous studies (Huang et al., 2014; Yuan et al., 2020). For each site, 31 samples and 23 species were input into PMF model. The number of samples is higher than the number of species. The input data include species concentration (including DTT_v, 14 trace elements and 8 organic markers) and uncertainties. The species-specific uncertainties were calculated following Liu et al. (2017). More details are described in SI (PMF analysis).

3 Results and discussion

3.1 DTT activity and concentrations of water-soluble PM$_{2.5}$ components

Figure 1 shows the daily variation of DTT activity, light absorption of WSOC at wavelength 365 nm (Abs$_{365}$), together with the concentrations of PM$_{2.5}$, WSOC, NACs and total elements in the south and north of Beijing. Their average values are shown in Table S1. Generally, the average values of PM$_{2.5}$, WSOC, Abs$_{365}$, NACs and total elements were higher in the south than in the north. Specifically, the concentrations of PM$_{2.5}$ and WSOC in the south (122 ± 49 μg m^{-3} and 8.1 ± 5.0 μgC m^{-3}, respectively) were both about two times higher than that in the north (62 ± 28 μg m^{-3} and 4.0 ± 2.0 μgC m^{-3}, respectively), indicating that the proportion of WSOC in PM$_{2.5}$ was similar in the south and north. However, the Abs$_{365}$ in the south was about three times that in the north, indicating that the chemical composition of WSOC was different between the south and north. Previous studies have reported that NACs are the main water-soluble light-absorbing organic compounds (also known as brown carbon, BrC) of PM$_{2.5}$ (Lin et al., 2017; Huang et al., 2020; Li et al., 2020). For the 7 NACs quantified in this study, the total concentration of nitrophenols (4NP, 2M4NP and 3M4NP), nitrocatechols (4NC, 3M5NC and 4M5NC), and 4N1N in the south (108 ± 73 ng m^{-3}, 118 ± 91 ng m^{-3} and 12 ± 8.2 ng m^{-3}, respectively) was about three, five and four times, respectively, those in the north (35 ± 22 ng m^{-3}, 24 ± 30 ng m^{-3}

and 3.1 ± 3.0 ng m^{-3}, respectively). These results indicate that the sources and emission strength of water-soluble organic compounds were different in the south and north of Beijing, suggesting the different contribution of water-soluble organic compounds to DTT activity. The concentration trends of trace elements were also different between the south and north of Beijing, with Fe > Zn > Ti > Mn > Cu > Ba > Pb > Sr > Cr > As > V > Ni > Cd > Co in the south, and Fe > Ti > Zn > Ba > Mn > Pb > Cu > Cr > Sr > As > Ni > V > Cd > Co in the north. It should be noted that although the contents of PM$_{2.5}$, WSOC and total elements measured in this study were higher in the south than in the north, the average DTT$_v$ value in the south (3.9 ± 0.9 nmol min^{-1} m^{-3}) was comparable to that in the north (3.5 ± 1.2 nmol min^{-1} m^{-3}), meanwhile, the average DTT$_m$ value was much higher (1.8 times) in the north (65 ± 28 pmol min^{-1} μg^{-1}) than in the south (36 ± 14 pmol min^{-1} μg^{-1}). The lower DTT$_m$ in the south than in the north may be due to the increased PM$_{2.5}$ in the south containing more substances with no or little contribution to DTT activity, and indicates that the intrinsic OP of water-soluble components of PM$_{2.5}$ was higher in the north than in the south. The similar DTT$_v$ values in the south and north indicate that the exposure-relevant OP of water-soluble components of PM$_{2.5}$ was comparable in the two sites, and the water-soluble DTT$_v$ was not consistent with the content of water-soluble substances.

Figure 2 shows the comparison of water-soluble PM$_{2.5}$ DTT activity measured in this study with those measured in other regions of Asia during similar periods. It can be seen that the DTT$_v$ values measured in Beijing in this study were lower than that in Jinzhou, Tianjin, Yantai, and Shanghai in China, Lahore and Peshawar in Pakistan, and Delhi in India (Liu et al., 2018; Ahmad et al., 2021; Puthussery et al., 2022; Wu et al., 2022a), higher than that in Xi'an, Nanjing, Hangzhou, Guangzhou, and Shenzhen in China (Wang et al., 2019; Wang et al., 2020b; Ma et al., 2021; Yu et al., 2022c; Xing et al., 2023), and comparable with that in Ningbo, China (Chen et al., 2022). Different from DTT$_v$, the DTT$_m$ value measured in NCNT in Beijing was similar with that in Jinzhou, Tianjin, Yantai, Shanghai and Ningbo in China (Liu et al., 2018; Chen

261 et al., 2022; Wu et al., 2022a), and higher than that in other regions. The differences in

262 water-soluble DTT activity of $PM_{2.5}$ in different regions can be explained by the

263 differences in chemical composition, sources and atmospheric formation processes

264 (Tong et al., 2017; Wong et al., 2019; Daellenbach et al., 2020; Wang et al., 2020b;

265 Cao et al., 2021). For example, Cao et al. (2021) reported the water-soluble DTT

266 activity of $PM_{2.5}$ from biomass and coal burning emissions in China, and the average

267 value of biomass burning (4.5-7.4 pmol min^{-1} μg^{-1}) was much higher than that of coal

268 burning (0.5-2.1 pmol min^{-1} μg^{-1}). Tuet et al. (2017) measured the water-soluble DTT

269 activity of SOA generated under different precursors and reaction conditions, with

270 SOA from naphthalene photooxidation under RO_2 + NO-dominant dry reaction

271 conditions had the highest DTT activity.

3.2 Correlation between DTT activity and water-soluble $PM_{2.5}$ components

273 Figure 3 shows the correlations of DTT_v with $PM_{2.5}$, WSOC and Abs_{365} in the

274 south and north of Beijing. It can be seen that the correlation coefficient between

275 DTT_v and $PM_{2.5}$ was moderate in both the south (r = 0.42) and north (r = 0.45),

276 indicating that the toxicity of particles cannot be evaluated solely by the total $PM_{2.5}$

277 concentration. The correlations between DTT_v with WSOC and Abs_{365} were strong in

278 the north (r of 0.69 and 0.70, respectively), while relatively weak in the south (r of

279 0.41 and 0.40, respectively). The high correlations between DTT_v with WSOC and

280 Abs_{365} in the north of Beijing qualitatively agree with previous studies in Xi'an, China

281 and Atlanta, United States (Verma et al., 2012; Chen et al., 2019), and suggest that

282 water-soluble organic matter, especially BrC, has a significant contribution to DTT

283 consumption in the north. Light-absorbing BrC typically has conjugated electrons,

284 making it more likely to transport electrons for catalytic reactions, thereby

285 contributing to DTT activity (Chen et al., 2019; Wu et al., 2022). Further, in the north,

286 the DTT_v was closely related to the concentrations of NACs (r of 0.57 to 0.79) (Figure

287 S3), suggesting that NACs may be important contributors to DTT consumption. Feng

288 et al. (2022) reported the positive correlations between NACs and biomarkers in

289 saliva and urine (interleukin-6 and 8-hydrox-2′-deoxyguanosine). Zhang et al. (2023)

also reported that NACs are major proinflammatory components in organic aerosols, contributing about 24% of the interleukin-8 response of all compounds detected by Fourier transform ion cyclotron resonance mass spectrometry (FT-ICR-MS) in electrospray ionization negative mode (ESI-). Certainly, it may also be other substances related to NACs that contribute to the DTT activity, including those not detected in this study, driving the good correlation between NACs and DTT_v in the north of Beijing, which is worth studying in the future.

The correlation coefficients between DTT_v and 14 trace elements are shown in Figure 4. Generally, the correlations between DTT_v and soluble elements were higher than that between DTT_v and total elements in both the south and north of Beijing. For soluble elements, in the south, the DTT_v showed positive correlations with Mn, Fe, Cr, Co, As and Pb ($r > 0.5$), while in the north, it exhibited strong positive correlations with Mn, Co, Ni, Zn, As, Cd and Pb ($r > 0.7$), indicating the different sources of DTT_v in the south and north of Beijing. It is worth noting that the concentrations of all soluble elements were higher in the south than in the north (Figure S4), while the correlation between DTT_v and most soluble elements was lower in the south than in the north (Figure 4). The high correlations between DTT_v and soluble elements in the north of Beijing suggests that soluble elements also had a significant contribution to DTT consumption. The low correlations between DTT_v and soluble elements in the south of Beijing may be due to the nonlinear relationship between DTT consumption and element concentration (Charrier and Anastasio, 2012; Wu et al., 2022a). As shown in Figure S5, the relationship between most soluble trace elements and DTT_v was more non-linear than linear. As the concentration of soluble elements increases, the growth rate of DTT_v obviously decreases.

In addition to being associated with individual water-soluble species, the interactions between metals and organic compounds also affect the consumption of DTT (Xiong et al., 2017; Wu et al., 2022b), with both synergistic and antagonistic effects. For example, Wu et al. (2022b) measured the DTT consumption of Fe(III) and Cu(II) interacting with 1,4-naphthoquinone, 9,10-phenanthraquinone, citric acid, and

319 4-nitrocatechol, respectively. Their results showed that Cu(II) had antagonistic effects

320 in interacting with most organics except for citric acid, and Fe(III) had an additive

321 effect on DTT consumption of 1,4-naphthoquinone and citric acid, while it had an

322 antagonistic effect on 1,4-naphthoquinone and 9,10-phenanthraquinone. Due to the

323 complex composition of water-soluble organic aerosols, the knowledge about the

324 effects of organics and metal-organic interactions on DTT activity are still limited,

325 especially the effects of BrC chromophores and their interactions with metals.

326 **3.3 Sources of DTT activity**

327 This study analyzed eight organic markers (including levoglucosan, mannosan,

328 and galactosan for biomass burning, hopanes for vehicle emissions, picene for coal

329 combustion, and phthalic acid, isophthalic acid and terephthalic acid for secondary

330 formation) to help identify the sources of DTT activity. The correlation coefficients

331 between DTT_v and organic markers are shown in Figure S6. In the south,

332 levoglucosan, mannosan, galactosan, and hopanes had moderate correlation with

333 DTT_v (r of 0.41 to 0.48); phthalic acid, isophthalic acid and terephthalic acid had low

334 to moderate correlation with DTT_v (r of 0.28 to 0.54); picene had low correlation with

335 DTT_v (r of 0.21). These results suggest that biomass burning and vehicle emissions

336 could have significant contribution to water-soluble $PM_{2.5}$ OP in the south. In the

337 north, hopanes had the highest correlation with DTT_v (r = 0.70), indicating that

338 vehicle emissions could have an important contribution. Levoglucosan, mannosan,

339 galactosan, phthalic acid, isophthalic acid, terephthalic acid, and picene had moderate

340 to high correlations with DTT_v in the north, suggesting that biomass and coal burning,

341 and secondary formation may also have certain contribution to water-soluble $PM_{2.5}$

342 OP.

343 To further quantify the sources of DTT activity in the south and the north of

344 Beijing, the PMF model, which was widely used for the source apportionment of

345 $PM_{2.5}$ OP (Liu et al., 2018; Shen et al., 2022; Cui et al., 2023), was applied. The input

346 species include DTT_v, soluble elements and organic markers, and five to seven factors

347 were examined. Due to the oil factor mixed with vehicle emissions factor in the five-

348 factor solution, and there was no new reasonable factor when increasing the factor

349 number to seven in the PMF analysis (Figure S7). Finally, six factors were resolved

350 and quantified using PMF model in the south and north of Beijing, including biomass

351 burning, coal burning, traffic-related, dust, oil combustion, and secondary formation,

352 and the profiles of these sources are shown in Figure S8. Factor 1 is characterized by

353 high contribution of levoglucosan, mannosan, and galactosan, mainly from biomass

354 burning (Huang et al., 2014; Chow et al., 2022). The DTT activity of biomass burning

355 organic aerosol was measured by Wong et al. (2019), which was 48 ± 6 pmol min^{-1}

356 μg^{-1} of WSOC. Liu et al. (2018) quantified the sources of DTT_v in coastal cities

357 (Jinzhou, Tianjin, and Yantai) in China with PMF model and multiple linear

358 regression method, and the results showed that biomass burning contributed 28% on

359 average in winter. Factor 2 exhibits a large fraction of picene, Zn, Mn, Cd, As, and Pb,

360 which is considered to be coal burning (Huang et al., 2014; Huang et al., 2018). Joo et

361 al. (2018) measured the DTT activity of $PM_{2.5}$ emitted from coal combustion at

362 different temperatures, with the highest values of 26 ± 21 pmol min^{-1} μg^{-1} and $0.10 \pm$

363 0.06 nmol min^{-1} m^{-3} occurring at 550 °C. Factor 3 is identified as traffic-related

364 emissions, which is characterized by the higher loading of hopanes, Ba, Sr, Cu and Ni

365 (Huang et al., 2018; Chow et al., 2022). Vreeland et al. (2017) measured the DTT

366 activity of $PM_{2.5}$ emitted by side street and highway vehicles in Atlanta, with values

367 of 0.78 ± 0.60 nmol min^{-1} m^{-3} and 1.1 ± 0.60 nmol min^{-1} m^{-3}, respectively. Ting et al.

368 (2023) reported that the DTT activity of $PM_{2.5}$ from vehicle emissions in Ziqing

369 tunnel in Taiwan, China, was 0.15-0.46 nmol min^{-1} m^{-3}. Factor 4, secondary formation,

370 which is identified by high levels of phthalic acid, isophthalic acid, and terephthalic

371 acid (Al-Naiema and Stone, 2017; Wang et al., 2020a). Verma et al. (2014) reported

372 that secondary formation contributed about 30% to the water-soluble DTT activity of

373 $PM_{2.5}$ in urban Atlanta. It is worth noting that the DTT activity of SOA generated

374 from different precursors is different (Tuet et al., 2017; Tong et al., 2018). For

375 example, the DTT activity of SOA from naphthalene was higher than that from

376 isoprene (Tuet et al., 2017; Tong et al., 2018). Factor 5 is dominated by crustal

377 elements Fe and Ti, mainly from dust (Huang et al., 2018). The DTT activity of

378 atmospheric particulate matter during dust periods were reported in previous studies

379 (Chirizzi et al., 2017; Khoshnamvand et al., 2023) and it has a low contribution in this

380 study. Factor 6 is identified as oil combustion because of the high levels of V and Ni

381 (Moreno et al., 2011; Minguillón et al., 2014; Huang et al., 2018).

382   The source contributions of DTT_v in the south and north of Beijing are shown in

383 Figure 5, exhibiting obvious district differences. In the south, traffic-related emissions

384 (39%) and biomass burning (25%) had the most contribution to DTT_v, followed by

385 secondary formation (17%), coal burning (15%), dust (2%), and oil combustion (2%).

386 In the north, traffic-related emissions (52%) had the highest contribution to DTT_v,

387 followed by coal burning (20%), secondary formation (13%), biomass burning (8%),

388 oil combustion (4%), and dust (3%). The absolute contribution of each source to

389 DTT_v varies by 1.2-3.4 times between the south and north of Beijing (Table S2). The

390 large district differences in sources of DTT_v of water-soluble $PM_{2.5}$ call for more

391 research on the relationship between sources, chemical composition, formation

392 processes and OP of $PM_{2.5}$.

393

394 **4 Conclusions**

395   In this study, the water-soluble OP of ambient $PM_{2.5}$ collected in winter in the

396 south and north of Beijing were quantified, together with the concentration and light

397 absorption of WSOC, and concentrations of 7 light-absorbing NACs and 14 trace

398 elements. The average DTT_v value was comparable in the south (3.9 ± 0.9 nmol min^{-1}

399 m^{-3}) and north (3.5 ± 1.2 nmol min^{-1} m^{-3}), while the DTT_m was higher in the north (65

400 ± 28 pmol min^{-1} μg^{-1}) than in the south (36 ± 14 pmol min^{-1} μg^{-1}), indicating that the

401 exposure-relevant OP of water-soluble components of $PM_{2.5}$ was similar in the two

402 sites and that the intrinsic OP of water-soluble components of $PM_{2.5}$ was higher in the

403 north than in the south. The correlation between DTT_v and soluble elements was

404 higher than that between DTT_v and total elements in both the south and north. In the

405 north, the DTT_v was strongly correlated with soluble Mn, Co, Ni, Zn, As, Cd and Pb

406   (r > 0.7), and in the south it positively correlated with Mn, Fe, Cr, Co, As and Pb (r >

407   0.5). In addition, in the north the DTT_v was also positively correlated with WSOC,

408   Abs_{365} and NACs (r of 0.56 to 0.79), while in the south it was weakly correlated (r $\leq$

409   0.4). These results indicate that in the north trace elements and water-soluble organic

410   compounds, especially BrC chromophores, both had significant contributions to DTT

411   consumption, and in the south the consumption of DTT may be mainly from trace

412   elements. Six sources of DTT_v were resolved with the PMF model, including biomass

413   burning, coal burning, traffic-related, dust, oil combustion, and secondary formation.

414   On average, traffic-related emissions (39%) and biomass burning (25%) were the

415   major contributors of DTT_v in the south, and traffic-related emissions (52%) was the

416   predominated source in the north. The differences in DTT_v sources in the south and

417   north of Beijing suggest that the relationship between source emissions and

418   atmospheric processes and $PM_{2.5}$ OP deserve further exploration in order to better

419   understand the regional differences of health impacts of $PM_{2.5}$.

420

421

422

423   **Date availability.** Raw data used in this study can be obtained from the following

424   open link: https://doi.org/10.5281/zenodo.10791126 (Yuan et al., 2024). It is also

425   available on request by contacting the corresponding author.

426

427   **Supplement.** The Supplement related to this article is available online.

428

429   **Author contributions.** RJH designed the study. Data analysis was done by WY, CL,

430   LY, HY and RJH. WY, CL, LY, HY and RJH interpreted data, prepared the display

431   items and wrote the manuscript. All authors commented on and discussed the

432   manuscript.

433

434   **Competing interests.** The authors declare that they have no conflict of interest.

Acknowledgements. We are very grateful to the National Natural Science Foundation of China (NSFC) under Grant No. 41925015, the Strategic Priority Research Program of Chinese Academy of Sciences (XDB40000000), the Key Research Program of Frontier Sciences from the Chinese Academy of Sciences (ZDBS-LY-DQC001), the New Cornerstone Science Foundation through the XPLORER PRIZE, and the Postdoctoral Fellowship Program of CPSF (no. GZC20232628) supported this study.

Financial support. This work was supported by the National Natural Science Foundation of China (NSFC) under Grant No. 41925015, the Strategic Priority Research Program of Chinese Academy of Sciences (XDB40000000), the Key Research Program of Frontier Sciences from the Chinese Academy of Sciences (ZDBS-LY-DQC001), the New Cornerstone Science Foundation through the XPLORER PRIZE, and the Postdoctoral Fellowship Program of CPSF (no. GZC20232628).

References

Ahmad, M., Yu, Q., Chen, J., Cheng, S., Qin, W., and Zhang, Y.: Chemical characteristics, oxidative potential, and sources of $PM_{2.5}$ in wintertime in Lahore and Peshawar, Pakistan, J. Environ. Sci., 102, 148-158, 10.1016/j.jes.2020.09.014, 2021.

Al-Naiema, I. M. and Stone, E. A.: Evaluation of anthropogenic secondary organic aerosol tracers from aromatic hydrocarbons, Atmos. Chem. Phys., 17, 2053-2065, 10.5194/acp-17-2053-2017, 2017.

An, Z., Huang, R. J., Zhang, R., Tie, X., Li, G., Cao, J., Zhou, W., Shi, Z., Han, Y., Gu, Z., and Ji, Y.: Severe haze in northern China: A synergy of anthropogenic emissions and atmospheric processes, Proc. Natl. Acad. Sci. U. S. A., 116, 8657-8666, 10.1073/pnas.1900125116, 2019.

Bates, J. T., Fang, T., Verma, V., Zeng, L., Weber, R. J., Tolbert, P. E., Abrams, J. Y., Sarnat, S. E., Klein, M., Mulholland, J. A., and Russell, A. G.: Review of Acellular Assays of Ambient Particulate Matter Oxidative Potential: Methods and Relationships with Composition, Sources, and Health Effects, Environ. Sci. Technol., 53, 4003-4019, 10.1021/acs.est.8b03430, 2019.

Burnett, R., Chen, H., Szyszkowicz, M., Fann, N., Hubbell, B., Pope, C. A., 3rd, Apte, J. S., Brauer, M., Cohen, A., Weichenthal, S., Coggins, J., Di, Q., Brunekreef, B., Frostad, J., Lim, S. S., Kan, H., Walker, K. D., Thurston, G. D., Hayes, R. B., Lim, C. C., Turner, M. C., Jerrett, M., Krewski, D., Gapstur, S. M., Diver, W. R., Ostro, B., Goldberg, D., Crouse, D. L., Martin, R. V., Peters, P., Pinault, L., Tjepkema, M., van Donkelaar, A., Villeneuve, P. J., Miller, A. B., Yin, P., Zhou, M., Wang, L., Janssen, N. A. H., Marra, M., Atkinson, R. W., Tsang, H., Quoc Thach, T., Cannon, J. B., Allen, R. T., Hart, J. E., Laden, F., Cesaroni, G., Forastiere, F., Weinmayr, G., Jaensch, A., Nagel, G., Concin, H., and Spadaro, J. V.: Global estimates of mortality associated with long-term exposure to outdoor fine particulate matter, Proc. Natl. Acad. Sci. U. S. A., 115, 9592-9597, 10.1073/pnas.1803222115, 2018.

Calas, A., Uzu, G., Kelly, F. J., Houdier, S., Martins, J. M. F., Thomas, F., Molton, F., Charron, A., Dunster, C., Oliete, A., Jacob, V., Besombes, J.-L., Chevrier, F., and Jaffrezo, J.-L.: Comparison between five acellular oxidative potential measurement assays performed with detailed chemistry on PM_{10} samples from the city of Chamonix (France), Atmos. Chem. Phys., 18, 7863-7875, 10.5194/acp-18-7863-2018, 2018.

Campbell, S. J., Wolfer, K., Utinger, B., Westwood, J., Zhang, Z. H., Bukowiecki, N., Steimer, S. S., Vu, T. V., Xu, J., Straw, N., Thomson, S., Elzein, A., Sun, Y., Liu, D., Li, L., Fu, P., Lewis, A. C., Harrison, R. M., Bloss, W. J., Loh, M., Miller, M. R., Shi, Z., and Kalberer, M.: Atmospheric conditions and composition that influence $PM_{2.5}$ oxidative potential in Beijing, China, Atmos. Chem. Phys., 21, 5549-5573, 10.5194/acp-21-5549-2021, 2021.

Cao, T., Li, M., Zou, C., Fan, X., Song, J., Jia, W., Yu, C., Yu, Z., and Peng, P. a.: Chemical composition, optical properties, and oxidative potential of water- and methanol-soluble organic compounds emitted from the combustion of biomass materials and coal, Atmos. Chem. Phys., 21, 13187-13205, 10.5194/acp-21-13187-2021, 2021.

Charrier, J. G. and Anastasio, C.: On dithiothreitol (DTT) as a measure of oxidative potential for ambient particles: evidence for the importance of soluble transition metals, Atmos. Chem. Phys., 12, 9321-9333, 10.5194/acp-12-9321-2012, 2012.

Charrier, J. G., McFall, A. S., Vu, K. K.-T., Baroi, J., Olea, C., Hasson, A., and Anastasio, C.: A Bias in the "Mass-Normalized" DTT Response-An Effect of Non-Linear Concentration Response Curves for Copper and Manganese, Atmos. Environ., 144, 325-334, 2016.

Chen, K., Xu, J., Famiyeh, L., Sun, Y., Ji, D., Xu, H., Wang, C., Metcalfe, S. E., Betha, R., Behera, S. N., Jia, C., Xiao, H., and He, J.: Chemical constituents, driving factors, and source apportionment of oxidative potential of ambient fine particulate matter in a Port City in East China, J. Hazard. Mater., 440, 10.1016/j.jhazmat.2022.129864, 2022.

Chen, Q., Wang, M., Wang, Y., Zhang, L., Li, Y., and Han, Y.: Oxidative Potential of Water-Soluble Matter Associated with Chromophoric Substances in $PM_{2.5}$ over Xi'an, China, Environ. Sci. Technol., 53, 8574-8584, 10.1021/acs.est.9b01976, 2019.

Chirizzi, D., Cesari, D., Guascito, M. R., Dinoi, A., Giotta, L., Donateo, A., and Contini, D.: Influence of Saharan dust outbreaks and carbon content on oxidative potential of water-soluble fractions of $PM_{2.5}$ and PM_{10}, Atmos. Environ., 163, 1-8, 10.1016/j.atmosenv.2017.05.021, 2017.

Chow, W. S., Huang, X. H. H., Leung, K. F., Huang, L., Wu, X., and Yu, J. Z.: Molecular and elemental marker-based source apportionment of fine particulate matter at six sites in Hong Kong, China, Sci. Total Environ., 813,

152652, 10.1016/j.scitotenv.2021.152652, 2022.

Chowdhury, P. H., He, Q., Carmieli, R., Li, C., Rudich, Y., and Pardo, M.: Connecting the Oxidative Potential of Secondary Organic Aerosols with Reactive Oxygen Species in Exposed Lung Cells, Environ. Sci. Technol., 53, 13949-13958, 10.1021/acs.est.9b04449, 2019.

Cui, Y., Zhu, L., Wang, H., Zhao, Z., Ma, S., and Ye, Z.: Characteristics and Oxidative Potential of Ambient $PM_{2.5}$ in the Yangtze River Delta Region: Pollution Level and Source Apportionment, Atmosphere, 14, 10.3390/atmos14030425, 2023.

Daellenbach, K. R., Uzu, G., Jiang, J., Cassagnes, L. E., Leni, Z., Vlachou, A., Stefenelli, G., Canonaco, F., Weber, S., Segers, A., Kuenen, J. J. P., Schaap, M., Favez, O., Albinet, A., Aksoyoglu, S., Dommen, J., Baltensperger, U., Geiser, M., El Haddad, I., Jaffrezo, J. L., and Prevot, A. S. H.: Sources of particulate-matter air pollution and its oxidative potential in Europe, Nature, 587, 414-419, 10.1038/s41586-020-2902-8, 2020.

Fan, X., Li, M., Cao, T., Cheng, C., Li, F., Xie, Y., Wei, S., Song, J., and Peng, P. a.: Optical properties and oxidative potential of water- and alkaline-soluble brown carbon in smoke particles emitted from laboratory simulated biomass burning, Atmos. Environ., 194, 48-57, 10.1016/j.atmosenv.2018.09.025, 2018.

Fang, T., Verma, V., Bates, J. T., Abrams, J., Klein, M., Strickland, M. J., Sarnat, S. E., Chang, H. H., Mulholland, J. A., Tolbert, P. E., Russell, A. G., and Weber, R. J.: Oxidative potential of ambient water-soluble $PM_{2.5}$ in the southeastern United States: contrasts in sources and health associations between ascorbic acid (AA) and dithiothreitol (DTT) assays, Atmos. Chem. Phys., 16, 3865-3879, 10.5194/acp-16-3865-2016, 2016.

Feng, R., Xu, H., Gu, Y., Wang, Z., Han, B., Sun, J., Liu, S., Lu, H., Ho, S. S. H., Shen, Z., and Cao, J.: Variations of Personal Exposure to Particulate Nitrated Phenols from Heating Energy Renovation in China: The First Assessment on Associated Toxicological Impacts with Particle Size Distributions, Environ. Sci. Technol., 56, 3974−3983, 2022.

551 Gao, D., Fang, T., Verma, V., Zeng, L., and Weber, R. J.: A method for measuring total
552   aerosol oxidative potential (OP) with the dithiothreitol (DTT) assay and
553   comparisons between an urban and roadside site of water-soluble and total OP,
554   Atmos. Meas. Tech., 10, 2821-2835, 10.5194/amt-10-2821-2017, 2017.

555 Hecobian, A., Zhang, X., Zheng, M., Frank, N., Edgerton, E. S., and Weber, R. J.:
556   Water-Soluble Organic Aerosol material and the light-absorption
557   characteristics of aqueous extracts measured over the Southeastern United
558   States, Atmos. Chem. Phys., 10, 5965-5977, 10.5194/acp-10-5965-2010, 2010.

559 Ho, K. F., Ho, S. S. H., Huang, R.-J., Liu, S. X., Cao, J.-J., Zhang, T., Chuang, H.-C.,
560   Chan, C. S., Hu, D., and Tian, L.: Characteristics of water-soluble organic
561   nitrogen in fine particulate matter in the continental area of China, Atmos.
562   Environ., 106, 252-261, 10.1016/j.atmosenv.2015.02.010, 2015.

563 Huang, R. J., Cheng, R., Jing, M., Yang, L., Li, Y., Chen, Q., Chen, Y., Yan, J., Lin, C.,
564   Wu, Y., Zhang, R., El Haddad, I., Prevot, A. S. H., O'Dowd, C. D., and Cao, J.:
565   Source-Specific Health Risk Analysis on Particulate Trace Elements: Coal
566   Combustion and Traffic Emission As Major Contributors in Wintertime
567   Beijing, Environ. Sci. Technol., 52, 10967-10974, 10.1021/acs.est.8b02091,
568   2018.

569 Huang, R. J., Yang, L., Shen, J., Yuan, W., Gong, Y., Guo, J., Cao, W., Duan, J., Ni, H.,
570   Zhu, C., Dai, W., Li, Y., Chen, Y., Chen, Q., Wu, Y., Zhang, R., Dusek, U.,
571   O'Dowd, C., and Hoffmann, T.: Water-Insoluble Organics Dominate Brown
572   Carbon in Wintertime Urban Aerosol of China: Chemical Characteristics and
573   Optical Properties, Environ. Sci. Technol., 54, 7836-7847,
574   10.1021/acs.est.0c01149, 2020.

575 Huang, R. J., Zhang, Y., Bozzetti, C., Ho, K. F., Cao, J. J., Han, Y., Daellenbach, K. R.,
576   Slowik, J. G., Platt, S. M., Canonaco, F., Zotter, P., Wolf, R., Pieber, S. M.,
577   Bruns, E. A., Crippa, M., Ciarelli, G., Piazzalunga, A., Schwikowski, M.,
578   Abbaszade, G., Schnelle-Kreis, J., Zimmermann, R., An, Z., Szidat, S.,
579   Baltensperger, U., El Haddad, I., and Prevot, A. S.: High secondary aerosol

contribution to particulate pollution during haze events in China, Nature, 514, 218-222, 10.1038/nature13774, 2014.

Jiang, H., Xie, Y., Ge, Y., He, H., and Liu, Y.: Effects of ultrasonic treatment on dithiothreitol (DTT) assay measurements for carbon materials, J. Environ. Sci., 84, 51–58, 2019.

Joo, H. S., Batmunkh, T., Borlaza, L. J. S., Park, M., Lee, K. Y., Lee, J. Y., Chang, Y. W., and Park, K.: Physicochemical properties and oxidative potential of fine particles produced from coal combustion, Aerosol Sci. Technol., 52, 1134-1144, 10.1080/02786826.2018.1501152, 2018.

Khoshnamvand, N., Nodehi, R. N., Hassanvand, M. S., and Naddafi, K.: Comparison between oxidative potentials measured of water-soluble components in ambient air PM_1 and $PM_{2.5}$ of Tehran, Iran, Air Qual. Atmos. Hlth., 16, 1311-1320, 10.1007/s11869-023-01343-y, 2023.

Laskin, A., Laskin, J., and Nizkorodov, S. A.: Chemistry of atmospheric brown carbon, Chem. Rev., 115, 4335-4382, 10.1021/cr5006167, 2015.

Lelieveld, S., Wilson, J., Dovrou, E., Mishra, A., Lakey, P. S. J., Shiraiwa, M., Poschl, U., and Berkemeier, T.: Hydroxyl Radical Production by Air Pollutants in Epithelial Lining Fluid Governed by Interconversion and Scavenging of Reactive Oxygen Species, Environ. Sci. Technol., 55, 14069-14079, 10.1021/acs.est.1c03875, 2021.

Lin, P., Bluvshtein, N., Rudich, Y., Nizkorodov, S. A., Laskin, J., and Laskin, A.: Molecular chemistry of atmospheric brown carbon inferred from a nationwide biomass burning event, Environ. Sci. Technol., 51, 11561–11570, 2017.

Liu, W., Xu, Y., Liu, W., Liu, Q., Yu, S., Liu, Y., Wang, X., and Tao, S.: Oxidative potential of ambient $PM_{2.5}$ in the coastal cities of the Bohai Sea, northern China: Seasonal variation and source apportionment, Environ. Pollut., 236, 514-528, 10.1016/j.envpol.2018.01.116, 2018.

Liu, Y., Yan, C. Q., Ding, X., Wang, X. M., Fu, Q. Y., Zhao, Q. B., Zhang, Y. H., Duan, Y. S., Qiu, X. H., and Zheng, M.: Sources and spatial distribution of

609   particulate polycyclic aromatic hydrocarbons in Shanghai, China, Sci. Total

610   Environ., 584-585, 307-317, https://doi.org/10.1016/j.scitotenv.2016.12.134,

611   2017.

612 Ma, X., Nie, D., Chen, M., Ge, P., Liu, Z., Ge, X., Li, Z., and Gu, R.: The Relative

613   Contributions of Different Chemical Components to the Oxidative Potential of

614   Ambient Fine Particles in Nanjing Area, Int. J. Environ. Res. Public Health, 18,

615   2789, 10.3390/ijerph18062789, 2021.

616 Miljevic, B., Hedayat, F., Stevanovic, S., Fairfull-Smith, K. E., Bottle, S. E., and

617   Ristovski, Z. D.: To sonicate or not to sonicate PM filters: reactive oxygen

618   species generation upon ultrasonic irradiation, Aerosol. Sci. Technol., 48,

619   1276-1284, 2014.

620 Minguillón, M. C., Cirach, M., Hoek, G., Brunekreef, B., Tsai, M., de Hoogh, K.,

621   Jedynska, A., Kooter, I. M., Nieuwenhuijsen, M., and Querol, X.: Spatial

622   variability of trace elements and sources for improved exposure assessment in

623   Barcelona, Atmos. Environ., 89, 268-281, 10.1016/j.atmosenv.2014.02.047,

624   2014.

625 Moreno, T., Querol, X., Alastuey, A., Reche, C., Cusack, M., Amato, F., Pandolfi, M.,

626   Pey, J., Richard, A., Prévôt, A. S. H., Furger, M., and Gibbons, W.: Variations

627   in time and space of trace metal aerosol concentrations in urban areas and their

628   surroundings, Atmos. Chem. Phys., 11, 9415-9430, 10.5194/acp-11-9415-2011,

629   2011.

630 Oh, S. H., Park, K., Park, M., Song, M., Jang, K. S., Schauer, J. J., Bae, G. N., and

631   Bae, M. S.: Comparison of the sources and oxidative potential of $PM_{2.5}$ during

632   winter time in large cities in China and South Korea, Sci. Total Environ., 859,

633   160369, 10.1016/j.scitotenv.2022.160369, 2023.

634 Paatero, P.: Least squares formation of robust non negative factor analysis,

635   Chemometr. Intell. Lab., 37, 23-35, 1997.

636 Puthussery, J. V., Dave, J., Shukla, A., Gaddamidi, S., Singh, A., Vats, P., Salana, S.,

637   Ganguly, D., Rastogi, N., Tripathi, S. N., and Verma, V.: Effect of Biomass

Burning, Diwali Fireworks, and Polluted Fog Events on the Oxidative Potential of Fine Ambient Particulate Matter in Delhi, India, Environ. Sci. Technol., 56, 14605-14616, 10.1021/acs.est.2c02730, 2022.

Shen, J., Taghvaee, S., La, C., Oroumiyeh, F., Liu, J., Jerrett, M., Weichenthal, S., Del Rosario, I., Shafer, M. M., Ritz, B., Zhu, Y., and Paulson, S. E.: Aerosol Oxidative Potential in the Greater Los Angeles Area: Source Apportionment and Associations with Socioeconomic Position, Environ. Sci. Technol., 56, 17795-17804, 10.1021/acs.est.2c02788, 2022.

Ting, Y. C., Chang, P. K., Hung, P. C., Chou, C. C., Chi, K. H., and Hsiao, T. C.: Characterizing emission factors and oxidative potential of motorcycle emissions in a real-world tunnel environment, Environ. Res., 234, 116601, 10.1016/j.envres.2023.116601, 2023.

Tong, H., Lakey, P. S. J., Arangio, A. M., Socorro, J., Kampf, C. J., Berkemeier, T., Brune, W. H., Poschl, U., and Shiraiwa, M.: Reactive oxygen species formed in aqueous mixtures of secondary organic aerosols and mineral dust influencing cloud chemistry and public health in the Anthropocene, Faraday Discuss., 200, 251-270, 10.1039/c7fd00023e, 2017.

Tong, H., Lakey, P. S. J., Arangio, A. M., Socorro, J., Shen, F., Lucas, K., Brune, W. H., Poschl, U., and Shiraiwa, M.: Reactive Oxygen Species Formed by Secondary Organic Aerosols in Water and Surrogate Lung Fluid, Environ. Sci. Technol., 52, 11642-11651, 10.1021/acs.est.8b03695, 2018.

Tuet, W. Y., Chen, Y., Xu, L., Fok, S., Gao, D., Weber, R. J., and Ng, N. L.: Chemical oxidative potential of secondary organic aerosol (SOA) generated from the photooxidation of biogenic and anthropogenic volatile organic compounds, Atmos. Chem. Phys., 17, 839-853, 10.5194/acp-17-839-2017, 2017.

Tuet, W. Y., Liu, F., de Oliveira Alves, N., Fok, S., Artaxo, P., Vasconcellos, P., Champion, J. A., and Ng, N. L.: Chemical Oxidative Potential and Cellular Oxidative Stress from Open Biomass Burning Aerosol, Environ. Sci. Technol. Lett., 6, 126-132, 10.1021/acs.estlett.9b00060, 2019.

Verma, V., Fang, T., Xu, L., Peltier, R. E., Russell, A. G., Ng, N. L., and Weber, R. J.: Organic aerosols associated with the generation of reactive oxygen species (ROS) by water-soluble $PM_{2.5}$, Environ. Sci. Technol., 49, 4646-4656, 10.1021/es505577w, 2015.

Verma, V., Rico-Martinez, R., Kotra, N., King, L., Liu, J., Snell, T. W., and Weber, R. J.: Contribution of water-soluble and insoluble components and their hydrophobic/hydrophilic subfractions to the reactive oxygen species-generating potential of fine ambient aerosols, Environ. Sci. Technol., 46, 11384-11392, 10.1021/es302484r, 2012.

Verma, V., Fang, T., Guo, H., King, L., Bates, J. T., Peltier, R. E., Edgerton, E., Russell, A. G., and Weber, R. J.: Reactive oxygen species associated with water-soluble $PM_{2.5}$ in the southeastern United States: spatiotemporal trends and source apportionment, Atmos. Chem. Phys., 14, 12915-12930, 10.5194/acp-14-12915-2014, 2014.

Vreeland, H., Weber, R., Bergin, M., Greenwald, R., Golan, R., Russell, A. G., Verma, V., and Sarnat, J. A.: Oxidative potential of $PM_{2.5}$ during Atlanta rush hour: Measurements of in-vehicle dithiothreitol (DTT) activity, Atmos. Environ., 165, 169-178, 10.1016/j.atmosenv.2017.06.044, 2017.

Wang, J., Lin, X., Lu, L., Wu, Y., Zhang, H., Lv, Q., Liu, W., Zhang, Y., and Zhuang, S.: Temporal variation of oxidative potential of water soluble components of ambient $PM_{2.5}$ measured by dithiothreitol (DTT) assay, Sci. Total Environ., 649, 969-978, 10.1016/j.scitotenv.2018.08.375, 2019.

Wang, T., Huang, R. J., Li, Y., Chen, Q., Chen, Y., Yang, L., Guo, J., Ni, H., Hoffmann, T., Wang, X., and Mai, B.: One-year characterization of organic aerosol markers in urban Beijing: Seasonal variation and spatiotemporal comparison, Sci. Total Environ., 743, 140689, 10.1016/j.scitotenv.2020.140689, 2020a.

Wang, Y., Wang, M., Li, S., Sun, H., Mu, Z., Zhang, L., Li, Y., and Chen, Q.: Study on the oxidation potential of the water-soluble components of ambient $PM_{2.5}$ over Xi'an, China: Pollution levels, source apportionment and transport pathways,

Environ. Int., 136, 105515, 10.1016/j.envint.2020.105515, 2020b.

Wong, J. P. S., Tsagkaraki, M., Tsiodra, I., Mihalopoulos, N., Violaki, K., Kanakidou, M., Sciare, J., Nenes, A., and Weber, R. J.: Effects of Atmospheric Processing on the Oxidative Potential of Biomass Burning Organic Aerosols, Environ. Sci. Technol., 53, 6747-6756, 10.1021/acs.est.9b01034, 2019.

Wu, N., Lu, B., Chen, Q., Chen, J., and Li, X.: Connecting the Oxidative Potential of Fractionated Particulate Matter With Chromophoric Substances, J. Geophys. Res-Atmos., 127, 10.1029/2021jd035503, 2022a.

Wu, N., Lyu, Y., Lu, B., Cai, D., Meng, X., and Li, X.: Oxidative potential induced by metal-organic interaction from $PM_{2.5}$ in simulated biological fluids, Sci. Total Environ., 848, 157768, 10.1016/j.scitotenv.2022.157768, 2022b.

Xing, C., Wang, Y., Yang, X., Zeng, Y., Zhai, J., Cai, B., Zhang, A., Fu, T. M., Zhu, L., Li, Y., Wang, X., and Zhang, Y.: Seasonal variation of driving factors of ambient $PM_{2.5}$ oxidative potential in Shenzhen, China, Sci. Total Environ., 862, 160771, 10.1016/j.scitotenv.2022.160771, 2023.

Xiong, Q., Yu, H., Wang, R., Wei, J., and Verma, V.: Rethinking Dithiothreitol-Based Particulate Matter Oxidative Potential: Measuring Dithiothreitol Consumption versus Reactive Oxygen Species Generation, Environ. Sci. Technol., 51, 6507-6514, 10.1021/acs.est.7b01272, 2017.

Yalamanchili, J., Hennigan, C. J., and Reed, B. E.: Measurement artifacts in the dithiothreitol (DTT) oxidative potential assay caused by interactions between aqueous metals and phosphate buffer, J. Hazard. Mater., 456, 131693, 2023.

Yu, H., Wei, J., Cheng, Y., Subedi, K., and Verma, V.: Synergistic and Antagonistic Interactions among the Particulate Matter Components in Generating Reactive Oxygen Species Based on the Dithiothreitol Assay, Environ. Sci. Technol., 52, 2261–2270, 2018.

Yu, Q., Chen, J., Qin, W., Ahmad, M., Zhang, Y., Sun, Y., Xin, K., and Ai, J.: Oxidative potential associated with water-soluble components of $PM_{2.5}$ in Beijing: The important role of anthropogenic organic aerosols, J. Hazard.

Mater., 433, 128839, 10.1016/j.jhazmat.2022.128839, 2022a.

Yu, S., Liu, W., Xu, Y., Yi, K., Zhou, M., Tao, S., and Liu, W.: Characteristics and oxidative potential of atmospheric $PM_{2.5}$ in Beijing: Source apportionment and seasonal variation, Sci. Total Environ., 650, 277-287, 10.1016/j.scitotenv.2018.09.021, 2019.

Yu, Y., Sun, Q., Li, T., Ren, X., Lin, L., Sun, M., Duan, J., and Sun, Z.: Adverse outcome pathway of fine particulate matter leading to increased cardiovascular morbidity and mortality: An integrated perspective from toxicology and epidemiology, J. Hazard. Mater., 430, 128368, 10.1016/j.jhazmat.2022.128368, 2022b.

Yu, Y., Cheng, P., Li, Y., Gu, J., Gong, Y., Han, B., Yang, W., Sun, J., Wu, C., Song, W., and Li, M.: The association of chemical composition particularly the heavy metals with the oxidative potential of ambient $PM_{2.5}$ in a megacity (Guangzhou) of southern China, Environ. Res., 213, 113489, 10.1016/j.envres.2022.113489, 2022c.

Yuan, W., Huang, R.-J., Luo, C., Yang, L., Cao, W., Guo, J., and Yang, H.: Measurement report: Oxidation potential of water-soluble aerosol components in the southern and northern of Beijing, Zenodo [data set], https://doi.org/10.5281/zenodo.10791126, 2024.

Yuan, W., Huang, R.-J., Yang, L., Guo, J., Chen, Z., Duan, J., Wang, T., Ni, H., Han, Y., Li, Y., Chen, Q., Chen, Y., Hoffmann, T., and O'Dowd, C.: Characterization of the light-absorbing properties, chromophore composition and sources of brown carbon aerosol in Xi'an, northwestern China, Atmos. Chem. Phys., 20, 5129-5144, 10.5194/acp-20-5129-2020, 2020.

Zhang, Q., Ma, H., Li, J., Jiang, H., Chen, W., Wan, C., Jiang, B., Dong, G., Zeng, X., Chen, D., Lu, S., You, J., Yu, Z., Wang, X., and Zhang, G.: Nitroaromatic Compounds from Secondary Nitrate Formation and Biomass Burning Are Major Proinflammatory Components in Organic Aerosols in Guangzhou: A Bioassay Combining High-Resolution Mass Spectrometry Analysis, Environ.

754   Sci. Technol., 57, 21570-21580, https://doi.org/10.1021/acs.est.3c04983, 2023.

755 Zheng, Y., Davis, S. J., Persad, G. G., and Caldeira, K.: Climate effects of aerosols

756   reduce economic inequality, Nat. Clim. Chang., 10, 220-224, 2020.

757

758

759

760
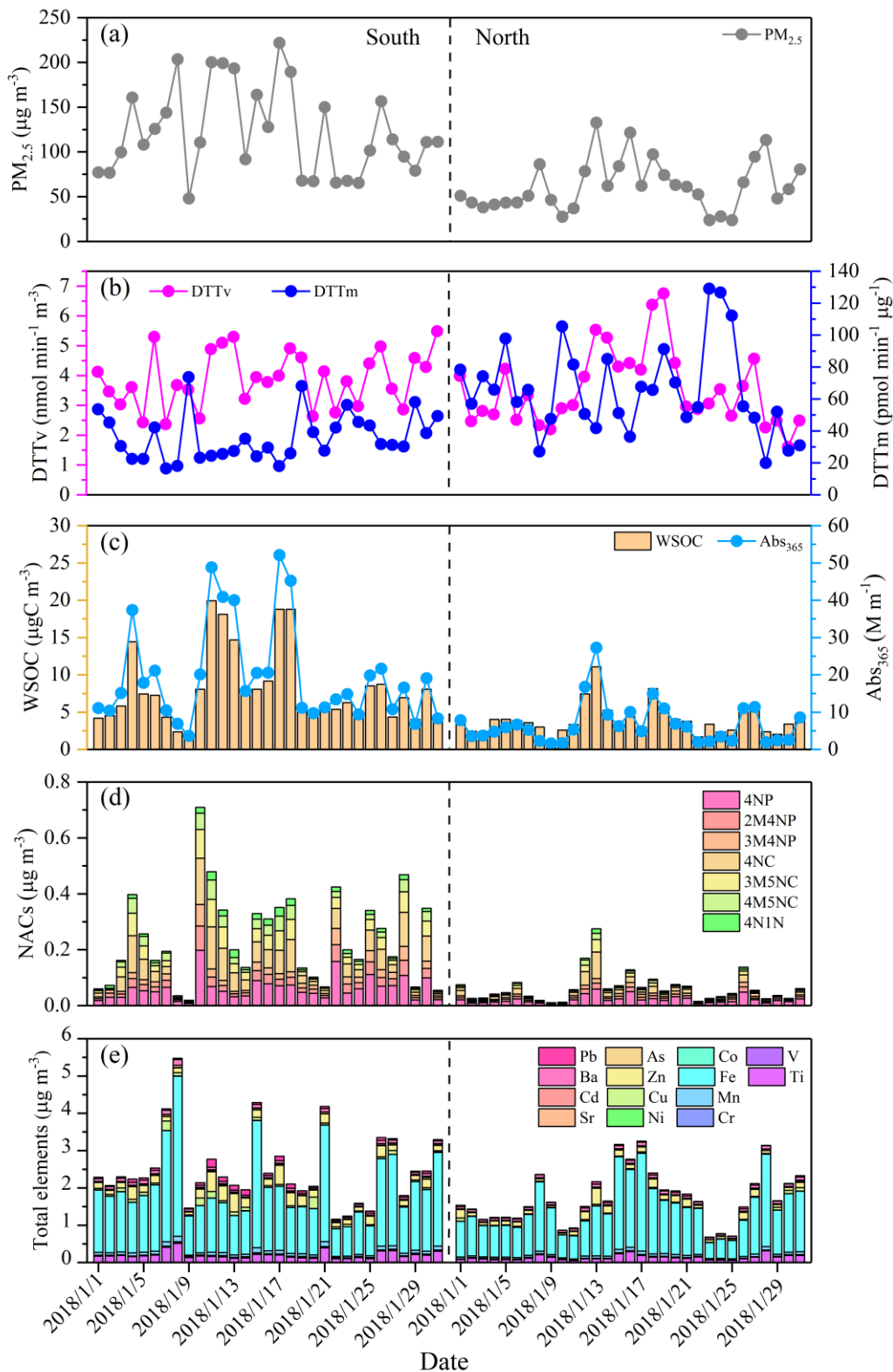
Figure 1. Time series of (a) PM$_{2.5}$ concentration, (b) DTT$_v$ and DTT$_m$, (c) concentration and light absorption at wavelength 365 nm (Abs$_{365}$) of WSOC, concentrations of (d) NACs and (e) elements.

765
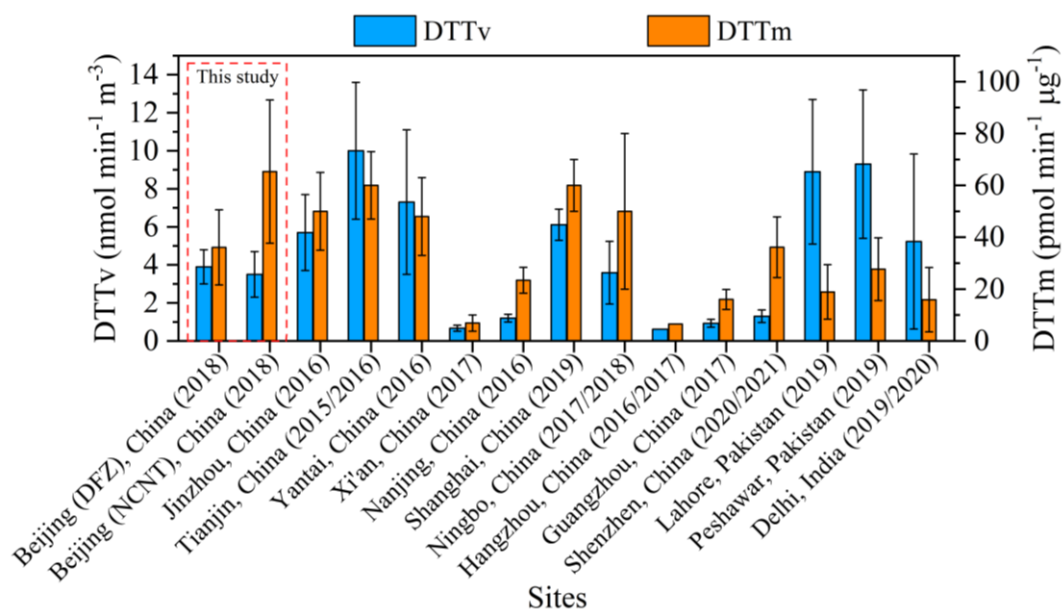
Figure 2. Comparison of DTT_v and DTT_m values of water-soluble $PM_{2.5}$ measured in

this study with those measured in other areas of Asia during similar period.

768

769
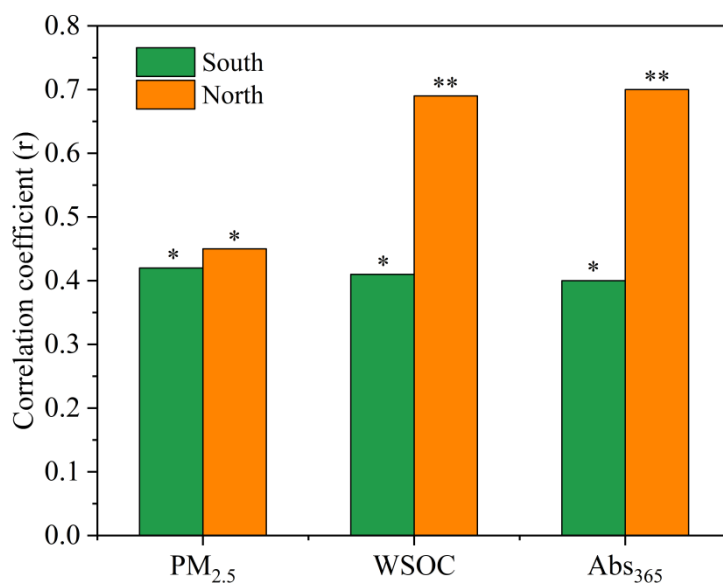
Figure 3. Correlation coefficients between DTT_v and $PM_{2.5}$, WSOC, and Abs_{365} in the

south and north of Beijing (* indicates correlation is significant at the 0.05 level, and

** indicates correlation is significant at the 0.01 level).

773

774
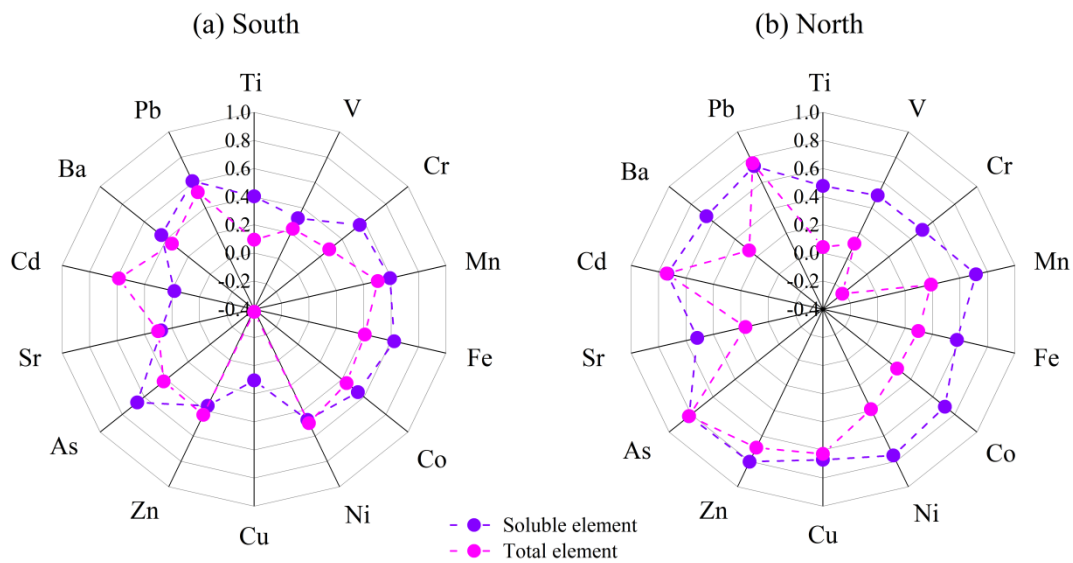
Figure 4. Correlation coefficients between DTT_v and elements in the (a) south and (b)

north of Beijing.

777

778
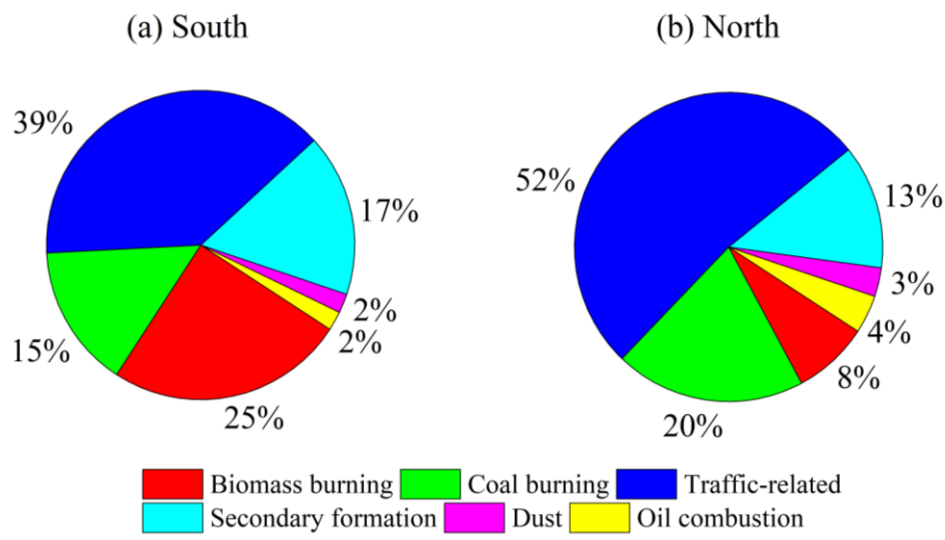
Figure 5. Contributions of resolved sources to DTT_v in the (a) south and (b) north of

Beijing.